Sum-Rate and Reliability Analysis for Power-Domain Non-Orthogonal Multiple Access (PD-NOMA)

Taehyeun Park*, Gilsoo Lee*, Walid Saad*, and Mehdi Bennis†
*Wireless@VT, Bradley Department of Electrical and Computer Engineering, Virginia Tech, Blacksburg, VA, USA,
† Centre for Wireless Communication, University of Oulu, Finland,
Emails:{taehyeun, gilsoolee, walids}@vt.edu, mehdi.bennis@oulu.fi.

***Abstract*—Non-orthogonal multiple access is seen as an important technology for tomorrow's Internet of Things (IoT) systems. In uplink power-domain non-orthogonal multiple access (PD-NOMA), allocating the uplink transmit power of the IoT devices is important to maximize both the sum-rate and the reliability of the devices. However, it is challenging to optimize the uplink transmit power when the received signal power is affected by a random fading channel. Hence, in this paper, the problem of uplink transmit power assignment is studied for a wireless network with PD-NOMA that serves uplink IoT services. This is posed as a problem of determining the target received signal power at the base station so that the reliability and the upper bound of sum-rate of the users are jointly maximized, where the received signal power at the base station is unknown to the devices due to Nakagami-m fading channel. To find an optimal allocation of the lower and higher target received power values for the devices using PD-NOMA, the reliability and the upper bound of sum-rate are derived in terms of target received power values and power difference threshold. For a special case of Nakagami-m fading channel, the theoretical analysis shows that the highest reliability and the highest upper bound of sum-rate are achieved, when the target received power values are highest. For a general Nakagami-m fading channel, simulation results show that there is a tradeoff between reliability and sum-rate upper bound and, thus, allocation of lower and higher target received power values is necessary to satisfy the communication requirements of IoT devices. Moreover, for a special case of Nakagami-m fading channel, simulation results show that the derived optimal transmit power achieves the optimal sum-rate upper bound and reliability, and the target received power values of two devices must be highest for the maximum upper bound of sum-rate and reliability. Furthermore, in simulation results, increasing the lower and higher target received power values increases both the upper bound of sum-rate and the reliability.**

***Index Terms*—Power-Domain non-orthogonal multiple access (PD-NOMA), Internet of Things Radio Resource Management.**

I. Introduction

Non-orthogonal multiple access (NOMA) can potentially improve spectral efficiency and, thus, it can be a suitable multiple access technology for emerging 6G systems and Internet of Things (IoT) [1]–[3]. In power-division (PD) NOMA, successive interference cancellation (SIC) is used by receivers to recover the transmitted signals from the superimposed, received signals [4]. To decode the received signals at the receiver, the value of the received signal powers should be different for successful SIC operation [5]. Therefore, if the signals from different devices are received with different power levels at the receiver, these multiple devices can be simultaneously supported over the same frequency spectrum at the same time. To determine the transmit power of the devices using PD-NOMA, designing effective transmit power allocation schemes for uplink radio resource management is essential to take advantage of SIC. In designing the transmit power allocation scheme for PD-NOMA, the sum-rate and reliability must be analyzed for PD-NOMA so that it can be practically used for IoT services requiring low latency and high reliability [3], [6].

This research was supported by the U.S. National Science Foundation under Grant CNS-1836802.

A. Related Works

In this regard, the transmit power allocation problem in the uplink of a NOMA system is studied in [7]–[19]. In particular, the data rate maximization problems of NOMA uplink systems are considered in [7], [9]–[12]. The work in [7] investigates a power allocation problem and shows the trade-off between orthogonal multiple access (OMA) and NOMA. In [8], the outage probability and the achievable average rate are investigated in downlink and uplink NOMA scenarios. The authors in [9] propose an uplink transmit power allocation scheme in which two users can simultaneously transmit their signals in each orthogonal subchannel. The work in [10] compares the sum-rate in uplink of a NOMA base station (BS) with the sum-rate of a conventional orthogonal multiple access (OMA) system when the BS is equipped with the multiple-input multiple-output (MIMO) infrastructure and uses millimeter-wave spectrum. The data rate of a two-user uplink NOMA system using a relay station is investigated in [11] when the relay has knowledge about its instantaneous fading channel. The authors in [12] show that the computational complexity of the average data rate maximization problem jointly optimizing subcarrier and power allocation in multi-carrier NOMA systems becomes NP-hard. Also, a number of problems related to the reliability of uplink NOMA systems are studied in [13] and [14]. The work in [13] investigates an uplink reliability improvement scheme that uses unscheduled transmissions with hybrid automatic request re-transmissions in NOMA systems. In [14], the theoretical transmission failure probability in NOMA uplink is derived to investigate the power

level partitioning problem of finding the minimum number of power levels used to transmit high-priority messages with minimum quality-of-service constraints. Furthermore, implementation and performance of NOMA for an IoT and its devices are studied in [15]–[19]. The authors in [15] propose a medium access control protocol for an IoT using NOMA to increase throughput. Moreover, the energy efficient resource allocation schemes for NOMA are analyzed for IoT devices with energy harvesting [16] and for mobile IoT devices [17]. The work in [18] proposes an intelligent clustering of mobile IoT devices in a cellular network with NOMA. Moreover, the authors in [19] discuss limitations and stability of deploying an IoT in cellular network with NOMA in terms of packet arrive rate, delay constraint and throughput.

In all of these existing NOMA works [7]–[19], it is generally assumed that the channel gains are known to the transmitting devices in a network. However, in practice, the uplink devices cannot have complete information on the instantaneous channels over the transmission time period, and, hence, the actual channel information can be uncertain particularly in a fading environment. This is particularly true in IoT system. Indeed, it is challenging for NOMA devices to control their uplink transmit power so that the received signal power at the BS is the target received power level. Further, most of existing works [7]–[19] investigate energy efficiency [16], [17], data rate [7]–[12], [15], [18], [19] or reliability [13], [14] as the main metrics interest of uplink NOMA systems. To achieve low latency and high reliability in PD-NOMA, the data rate and reliability can be jointly optimized. Consequently, unlike the existing literature [7]–[14] which assumes full information knowledge for channel in NOMA uplink and optimizes a single objective, our goal is to design an uplink transmit power allocation scheme for NOMA, under uncertainty on fading channels, while maximizing both the sum-rate upper bound and the reliability of the uplink devices in a wireless PD-NOMA network. These considerations are particularly suitable for IoT systems.

B. Key Contributions

The main contribution of this paper is a novel analytical framework for optimal uplink transmit power allocation that maximizes the sum-rate upper bound and the reliability of the devices in a NOMA wireless system that must meet reliability targets for IoT-like services. This framework allows a BS to allocate the optimal target received power values to the devices using PD-NOMA. The BS needs to allocate the uplink transmit power values to the devices so that the separation of actual received power levels at the BS is greater than the power difference threshold required for SIC operation. When the transmitting devices do not know the exact channel gains due to random channel fading, we formulate a multi-objective optimization problem whose objective is to maximize the reliability and the upper bound of sum-rate, which are critical performance metrics for IoT services. To solve this problem, we analyze the sum-rate upper bound and the reliability in terms of target received power values and power threshold. Also, for Rayleigh fading channel, we show that both the sum-rate upper bound and the reliability are increasing functions of the target received power values, and the reliability is a decreasing function of the power difference threshold. Therefore, for the case in which there are two devices using PD-NOMA under Rayleigh fading channel, mathematical analysis shows that the highest sum-rate upper bound and the highest reliability are achieved when the target received power values are highest. Simulation results confirm the theoretical results and show that the proposed transmit power allocation scheme maximizes the sum-rate upper bound and reliability. Therefore, with Rayleigh fading channel, the proposed framework is shown to be able to achieve the optimal sum-rate upper bound and reliability of the devices by allocating the highest value of the target received power values of two devices. However, with Nakagami-m fading channel, simulation results show that there is a tradeoff between sum-rate upper bound and reliability depending on the target received power values, and, thus, an uplink transmit power allocation is necessary to satisfy the communication requirements of IoT-like services. For a specific simulation setting, simulation results also show that decreasing the power difference threshold is more effective in increasing the reliability than increasing the target received power values.

The rest of this paper is organized as follows. In Section II, we present the system model. In Section III, we analyze the performance of allocating uplink transmit power for the uplink users and prove that the derived transmit power allocation scheme achieves the optimal sum-rate upper bound and reliability. Simulation results are analyzed in Section IV while conclusions are drawn in Section V.

II. System Model

Consider the uplink of a wireless system consisting of one BS located at the center of a geographical area in which two devices are active. Those devices can be seen as IoT-like devices that need to transmit uplink data reliably and within a short deadline. For the communication between a device and the BS, we consider a time-slotted system with time slot duration of τ using a PD-NOMA scheme with two adjustable power levels. The two adjustable power levels include a lower target received power t_l and a higher target received power t_h such that $t_l \leq t_h$. In PD-NOMA, the two devices choose different target received power levels and transmit simultaneously so that the BS can decode the received signals using SIC. We assume that target received power values t_l and t_h are assigned to the two devices by the BS and that the two devices know their target received power values. Without loss of generality, we let device l be a device assigned with t_l and device h be a device assigned with t_h.

We consider a Nakagami-m fading channel and path loss with parameters α_1 and α_2. We assume that the devices only know the parameter of the Nakagami fading channel m and their distances to the BS. We let d_l be the distance between

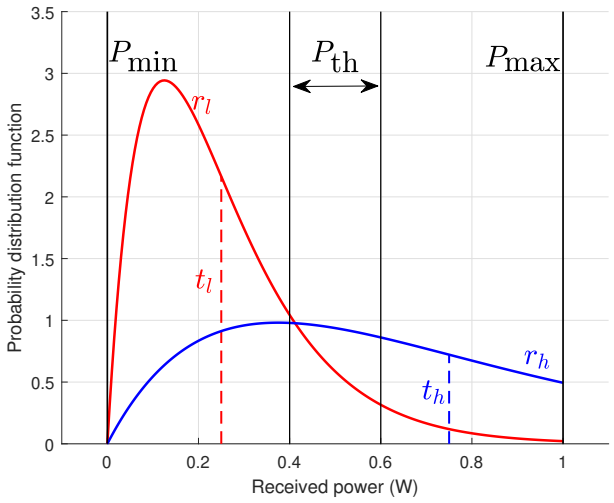

Fig. 1: A model explaining the relations between the key parameters of the system model with $t_l = 0.25$ W, $t_h = 0.75$ W, $m = 2$, $P_{\min} = 0$ W, $P_{\max} = 1$ W, and $P_{\text{th}} = 0.2$ W.

the BS and device l and d_h be the distance between the BS and device h. The actual received power r_i by device i for $i \in \{l, h\}$ will be:

$$r_i = L_i p_i g, \tag{1}$$

$$L_i = \alpha_2 d_i^{-\alpha_1}, \tag{2}$$

where g is the Nakagami fading channel gain, L_i is the path loss of device i, and p_i is transmit power of device i. Since the devices know m and their distances d_i to the BS, the devices can adjust their transmit power values p_i such that the expected received power values $\mathbb{E}[r_i]$ match their assigned target received power levels t_i.

The mathematical analysis of sum-rate upper bound and reliability is done for a Nakagami-m fading channel with $m = 1$, which is equivalent to a Rayleigh fading channel. Although the received power with Nakagami fading channel is gamma distributed and the theoretical analysis is mathematically intractable, the received power with Rayleigh fading channel is exponentially distributed with mean λ^{-1}. Considering p_i to be constant and with known d_i, the actual received power r_i is random due to g, and the expected value of r_i should be equal to t_i such that:

$$\mathbb{E}[r_i] = t_i = \mathbb{E}[L_i p_i g] = \frac{p_i \alpha_2 d_i^{-\alpha_1}}{\lambda}, \tag{3}$$

$$p_i = \frac{\lambda t_i}{\alpha_2 d_i^{-\alpha_1}}, \tag{4}$$

$$r_i = \alpha_2 d_i^{-\alpha_1} \left(\frac{\lambda t_i}{\alpha_2 d_i^{-\alpha_1}} \right) g = \lambda t_i g. \tag{5}$$

The long term transmit power allocation p_i in (4) is a value of transmit power to ensure that $\mathbb{E}[r_i] = t_i$ by considering the known λ and d_i. Since g is exponentially distributed with mean λ^{-1}, r_i in (5) is also exponentially distributed with mean t_i. Figure 1 shows an example of r_l and r_h with given t_l, t_h, m, $P_{\min}$, $P_{\max}$, and P_{th}.

The target received power values t_l and t_h are within the bounds of $P_{\min}$ and $P_{\max}$ such that $t_l, t_h \in [P_{\min}, P_{\max}]$. We let P_{range} be a range of power that t_l and t_h are in such that $P_{\text{range}} = (P_{\max} - P_{\min})$. The values of t_l and t_h must be chosen carefully as the received signals are decoded using SIC. The SIC cannot decode the received signals if the difference of the received power values Δ_r is less than or equal to a power difference threshold P_{th}, which can be affected by the SIC and the device rate requirement [5]. In other words, for PD-NOMA, a transmission will fail if the difference between the actual received power values $\Delta_r = |r_h - r_l|$ is less than or equal to P_{th}. Typically, P_{th} is within the bounds of 0 and $(P_{\max} - P_{\min})$, and a smaller P_{th} implies better performing SIC. Moreover, the probability of transmission failure is defined as $\Pr(\Delta_r \leq P_{\text{th}})$. In our model, the *reliability* S is defined as the probability of successful transmission, which is $S = 1 - \Pr(\Delta_r \leq P_{\text{th}})$. This is a key parameter for IoT-like services that must deliver data reliably to the BS. Our definition of reliability S is similar to the definition of reliability based on SINR, because high interference implies that Δ_r is more likely to be small and results in low reliability. Furthermore, when a transmission is successful, the achievable expected sum-rate R_o of the two devices each targeting t_l and t_h is:

$$R_o = \mathbb{E}\left[B \log_2 \left(1 + \frac{r_h}{r_l + \sigma^2} \right) + B \log_2 \left(1 + \frac{r_l}{\sigma^2} \right) \right], \tag{6}$$

where B is the bandwidth and σ^2 is the additive white Gaussian noise power. Since r_l and r_h are both random variables, closed-form derivation and mathematical analysis of R_o is intractable. Therefore, an upper bound R for the achievable expected sum-rate R_o will be analyzed, and R is:

$$R = \mathbb{E}\left[\sum_{i \in \{l,h\}} B \log_2 \left(1 + \frac{r_i}{\sigma^2} \right) \right]. \tag{7}$$

If the difference between t_h and t_l is bigger, the interference from device l to device h is smaller, and, thus, the achievable expected sum-rate R_o approaches the upper bound R. Since PD-NOMA is a promising multiple access scheme for IoT services, the performance of PD-NOMA in terms of sum-rate upper bound and reliability will be further analyzed. Therefore, a multi-objective optimization problem maximizing the sum-rate upper bound R and the reliability S can be formulates such that:

$$\max_{t_l, t_h} \quad (S, R), \tag{8}$$

$$\text{s.t.} \quad P_{\min} \leq t_l \leq t_h \leq P_{\max}. \tag{9}$$

In the following section, we will find the optimal solution that maximizes both the reliability S and the sum-rate upper bound R.

III. Performance Analysis

For PD-NOMA to be used for certain IoT-like services, such as remote control of autonomous vehicles for vehicle-to-everything network [20] and virtual reality (which is part of a future Internet of Everything system) [21], a highly reliable communication and a timely transmission are required. Therefore, it is essential to determine how the sum-rate and the reliability are affected by the system parameters. In particular, the sum-rate upper bound and the reliability of PD-NOMA will be analyzed as functions of the lower target received power t_l, the higher power received power t_h, and the power difference threshold P_{th}.

A. PD-NOMA Reliability

In our system model, the transmissions using PD-NOMA from both devices fail if $\Delta_r \leq P_{\text{th}}$ and SIC fails to decode the received signals. Therefore, the reliability S is defined as the probability that SIC can successfully decode the received signals and transmission do not fail, which is:

$$S = 1 - \Pr(\Delta_r \leq P_{\text{th}}). \tag{10}$$

Proposition 1. For two devices using PD-NOMA with target received power values t_l and t_h and SIC failing to decode if the difference of the received power values is less than or equal to a power difference threshold P_{th}, the reliability S is:

$$S = \frac{t_h}{t_l + t_h} e^{-P_{\text{th}}/t_h} + \frac{t_l}{t_l + t_h} e^{-P_{\text{th}}/t_l}. \tag{11}$$

Proof. For a random fading channel g, the actual received powers r_l and r_h are random. Therefore, in a given time slot, the actual received powers must be one of the two cases, which are $r_h \geq r_l$ and $r_l \geq r_h$.

For the first case where $r_h \geq r_l$, we let s_1 be $r_h - r_l$ and $s_1 \geq 0$. s_1 is a difference between two exponential distributions r_h and r_l with means t_h and t_l, respectively. Therefore, the probability density function of s_1 is:

$$f_{s_1}(x) = \frac{1}{t_l + t_h} \begin{cases} e^{-x/t_h} & \text{if } x \geq 0, \\ e^{x/t_l} & \text{if } x < 0. \end{cases} \tag{12}$$

For the first case, the probability of transmission failure is:

$$\Pr(|r_h - r_l| \leq P_{\text{th}}) = \Pr(r_h - r_l \leq P_{\text{th}}) = \Pr(s_1 \leq P_{\text{th}}), \tag{13}$$

$$= \int_0^{P_{\text{th}}} f_{s_1}(x)dx = \int_0^{P_{\text{th}}} \frac{1}{t_l + t_h} e^{-x/t_h} dx, \tag{14}$$

$$= \frac{t_h}{t_l + t_h} \left(1 - e^{-P_{\text{th}}/t_h}\right). \tag{15}$$

Similarly, for the second case where $r_l \geq r_h$, we let s_2 be $r_l - r_h$ and $s_2 \geq 0$. The probability density function of s_2 is:

$$f_{s_2}(x) = \frac{1}{t_l + t_h} \begin{cases} e^{-x/t_l} & \text{if } x \geq 0, \\ e^{x/t_h} & \text{if } x < 0, \end{cases} \tag{16}$$

which is the probability density function of s_1 reflected about y-axis. Moreover, the probability of transmission failure for the second case is:

$$\Pr(|r_h - r_l| \leq P_{\text{th}}) = \Pr(r_l - r_h \leq P_{\text{th}}) = \Pr(s_2 \leq P_{\text{th}}), \tag{17}$$

$$= \int_0^{P_{\text{th}}} f_{s_2}(x)dx = \int_0^{P_{\text{th}}} \frac{1}{t_l + t_h} e^{-x/t_l} dx, \tag{18}$$

$$= \frac{t_l}{t_l + t_h} \left(1 - e^{-P_{\text{th}}/t_l}\right). \tag{19}$$

The total probability of transmission failure is:

$$\Pr(\Delta_r \leq P_{\text{th}}) = \Pr(|r_h - r_l| \leq P_{\text{th}}) \tag{20}$$

$$= \Pr(r_h - r_l \leq P_{\text{th}}) + \Pr(r_l - r_h \leq P_{\text{th}}) \tag{21}$$

$$= 1 - \frac{t_h}{t_l + t_h} e^{-P_{\text{th}}/t_h} - \frac{t_l}{t_l + t_h} e^{-P_{\text{th}}/t_l}. \tag{22}$$

Therefore, the reliability S of our system model is:

$$S = \frac{t_h}{t_l + t_h} e^{-P_{\text{th}}/t_h} + \frac{t_l}{t_l + t_h} e^{-P_{\text{th}}/t_l}. \tag{23}$$

■

Since P_{th} is a given system parameter and the reliability S in (11) is a function of t_l, t_h, and P_{th}, it is essential to analyze S in terms of t_l and t_h to find an optimal solution to the maximization problem in (8).

Proposition 2. For some fixed values of $P_{\min} \geq 0$, $P_{\max} > 0$, $t_h \in [P_{\min}, P_{\max}]$, and $P_{\text{th}} \geq 0$, the highest achievable reliability is:

$$\max_{t_l} S = e^{-P_{\text{th}}/t_h}, \tag{24}$$

and this is achieved when $t_l = 0$ or $t_l = t_h$ if $P_{\min} = 0$ and only when $t_l = t_h$ if $P_{\min} > 0$.

Proof. By the definition of t_l, $t_l \in [P_{\min}, P_{\max}]$ and $t_h \geq t_l$. At the bounds of t_l, when $t_l = 0$ and $t_l = t_h$, the value of reliability function is e^{-P_{th}/t_h}. For any value of $t_l = \beta$ such that $\beta \in (0, t_h)$, the value of reliability function is always less than the value of reliability function at the bounds of t_l such that:

$$e^{-P_{\text{th}}/t_h} > \frac{t_h}{\beta + t_h} e^{-P_{\text{th}}/t_h} + \frac{\beta}{\beta + t_h} e^{-P_{\text{th}}/\beta}, \tag{25}$$

$$e^{-P_{\text{th}}/t_h} > e^{-P_{\text{th}}/\beta}. \tag{26}$$

Since $t_h > \beta$, e^{-P_{th}/t_h} is always less than $e^{-P_{\text{th}}/\beta}$. Therefore, the highest value of reliability is e^{-P_{th}/t_h} when $t_l = 0$ or $t_l = t_h$ if $P_{\min} = 0$ and only when $t_l = t_h$ if $P_{\min} > 0$. ■

When $t_l = 0$, the reliability is highest. However, this also implies that device l is not served, and the transmission from device h fails only due to severe Rayleigh fading. Moreover, the sum-rate of the devices will be greatly reduced when $t_l = 0$ and device l is not served.

For a fixed value of $t_h \in [P_{\min}, P_{\max}]$, the highest achievable

reliability is e^{-P_{th}/t_h} (24). This is an increasing function of t_h, and the highest reliability S for any $t_l, t_h \in [P_{\min}, P_{\max}]$ is:

$$\max_{t_l,t_h} S = e^{-P_{\text{th}}/P_{\max}}, \tag{27}$$

which occurs when $t_l = t_h = P_{\max}$. This is because the target received power t_i is the mean of exponentially distributed actual received power r_i for $m = 1$. As t_i increases, variance of r_i also increases, because the variance of r_i is t_i^2. Therefore, it is more likely for the actual received powers to be separated by more than P_{th} as t_i increases. Next, the second part of the optimization problem maximizing the sum-rate upper bound in (8) will be analyzed.

B. PD-NOMA Sum-Rate

The sum-rate of PD-NOMA is of interest as the sum-rate will affect the latency of the transmission. The sum-rate upper bound R of the two devices each targeting t_l and t_h is:

$$R = \mathbb{E}\left[\sum_{i\in\{l,h\}} B\log_2\left(1+\frac{r_i}{\sigma^2}\right)\right]. \tag{28}$$

Proposition 3. For two devices using PD-NOMA with target received power values t_l and t_h, the sum-rate upper bound R is:

$$R = \frac{-B}{\ln(2)}\sum_{i\in\{l,h\}} \exp\left(\frac{\sigma^4}{t_i}\right)\text{Ei}\left(\frac{-\sigma^4}{t_i}\right), \tag{29}$$

where $\text{Ei}(x)$ is an exponential integral function.

Proof. The actual received power values r_l and r_h are exponentially distributed with means t_l and t_h, respectively. Therefore, for $i \in \{l, h\}$, $\frac{r_i}{\sigma^2}$ is exponentially distributed with mean $\frac{t_i}{\sigma^2}$. Therefore, the sum-rate upper bound is:

$$\sum_{i\in\{l,h\}}\int_0^\infty B\log_2\left(1+\frac{r_i}{\sigma^2}\right)\frac{\sigma^2}{t_i}\exp\left(\frac{-r_i\sigma^2}{t_i}\right)dr_i$$

$$= \frac{B}{\ln(2)}\sum_{i\in\{l,h\}}\int_0^\infty \ln\left(1+\frac{r_i}{\sigma^2}\right)\frac{\sigma^2}{t_i}\exp\left(\frac{-r_i\sigma^2}{t_i}\right)dr_i.$$

Substituting $t = 1 + \frac{r_i}{\sigma^2}$, the sum-rate upper bound is:

$$\frac{B\sigma^2}{\ln(2)}\sum_{i\in\{l,h\}}\frac{1}{t_i}\int_1^\infty \ln(t)\exp\left(\frac{(1-t)\sigma^4}{t_i}\right)\sigma^2 dt$$

$$= \frac{B\sigma^4}{\ln(2)}\sum_{i\in\{l,h\}}\frac{\exp(\sigma^4/t_i)}{t_i}\int_1^\infty \ln(t)\exp\left(\frac{-\sigma^4 t}{t_i}\right)dt.$$

Using integral solution from [22, Equation (4.331-2)], the sum-rate upper bound becomes:

$$\frac{B\sigma^4}{\ln(2)}\sum_{i\in\{l,h\}}\frac{\exp(\sigma^4/t_i)}{t_i}\left(\frac{-t_i}{\sigma^4}\text{Ei}\left(\frac{-\sigma^4}{t_i}\right)\right)$$

$$= \frac{-B}{\ln(2)}\sum_{i\in\{l,h\}}\exp\left(\frac{\sigma^4}{t_i}\right)\text{Ei}\left(\frac{-\sigma^4}{t_i}\right).$$

■

Since $\text{Ei}(0) = -\infty$ and $\text{Ei}(x) = 0$ as x approaches $-\infty$, $\text{Ei}\left(-\sigma^4/t_i\right)$ is a strictly decreasing function of t_i. As t_i increases, $\exp\left(\sigma^4/t_i\right)$ approaches 1, while $\text{Ei}\left(-\sigma^4/t_i\right)$ approaches $-\infty$. Therefore, the sum-rate upper bound is an increasing function of t_i.

Similar to the highest reliability in (27), the highest sum-rate upper bound is:

$$\max_{t_l,t_h} R = \frac{-2B}{\ln(2)}\exp\left(\frac{\sigma^4}{P_{\max}}\right)\text{Ei}\left(\frac{-\sigma^4}{P_{\max}}\right), \tag{30}$$

which occurs when $t_l = t_h = P_{\max}$. Since the highest sum-rate upper bound and the highest reliability are both achieved when $t_l = t_h = P_{\max}$, the optimal solution to the maximization problem in (8) is $t_l = t_h = P_{\max}$. One implication of this result is that the two devices should choose the target received power of $P_{\max}$ for highest sum-rate upper bound and reliability for the case of two devices using PD-NOMA. Moreover, it is unnecessary for the BS to allocate the lower and higher target received power values t_l and t_h to the devices.

The solution of $t_l = t_h = P_{\max}$ to optimization problem (8) is only limited to Rayleigh fading channels. This is because the received power (5) is exponentially distributed with Rayleigh fading channel, and the variance of received power increases with higher target received power. Therefore, with higher variance, it is more likely for the actual received signal powers to be separated by more than P_{th} for successful transmission. Furthermore, with a higher target received power, the actual received power increases, and, thus, the sum-rate increases.

For a general Nakagami-m fading channel with $m > 1$, the optimization problem in (8) does not admit the solution of $t_l = t_h = P_{\max}$, because the received power is gamma distributed. Unlike an exponential distribution that has a peak at 0, a gamma distribution with $m > 1$ does not have a peak at 0 as shown in Figure 1, and a peak of gamma distribution changes depending on the target received power. As t_l increases to t_h, the actual received powers r_l and r_h eventually have same nonzero peaks, and, thus, it is less likely for r_l and r_h to be separated by more than P_{th} for successful transmission. In other words, as t_l increases to t_h, the sum-rate increases, while the reliability decreases. Therefore, there is a tradeoff between sum-rate and reliability as t_l increases to t_h, and $t_l = t_h = P_{\max}$ is not a solution to optimization problem with $m > 1$. The tradeoff between sum-rate and reliability with $m > 1$ is further analyzed via simulations in Section IV.

IV. Simulation Results and Analysis

For our simulations, we focus on analyzing the rate and the reliability of the PD-NOMA for various lower target received power t_l, higher target received power t_h, power range P_{range}, and power different threshold P_{th}. For SIC, the maximum power $P_{\max}$ is set to 1 W, and the minimum power $P_{\min}$ is set to 0 W, which means that the power range P_{range} is set to 1 W. For all simulations, we determine the values of t_l, t_h,

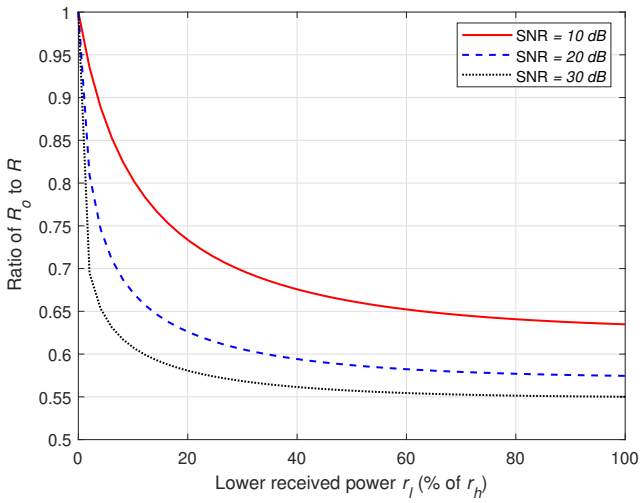

Fig. 2: Ratio of achievable expected sum-rate to sum-rate upper bound for various values of r_l and SNR with $r_h = P_{\max}$.

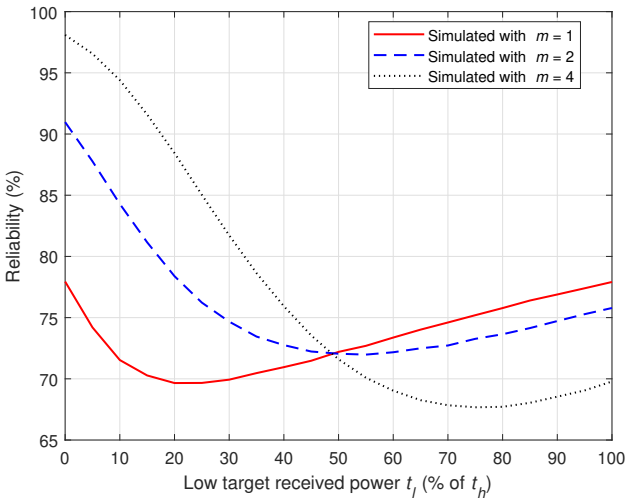

Fig. 3: Simulated reliability for various values of t_l and m with $t_h = P_{\max}$ and $P_{\text{th}} = 25\%$ of P_{range}.

and P_{th} as the percentages of either $P_{\max}$ and P_{range}. Since the sum-rate upper bound (29) and the reliability (11) are functions of t_l, t_h, and P_{th}, the simulation results are valid for different values of $P_{\min}$ and $P_{\max}$ as long as the relative values of t_l, t_h, and P_{th} with respect to $P_{\min}$ and $P_{\max}$ are the same. For instance, the simulation result for $P_{\text{th}} = 0.1$ W with $P_{\max} = 1$ W is equivalent to the simulation result for $P_{\text{th}} = 0.01$ W with $P_{\max} = 0.1$ W. Therefore, the simulation results can be readily used to analyze the sum-rate upper bound and the reliability of PD-NOMA with various values of $P_{\min}$ and $P_{\max}$.

In our simulations, we set the noise power to -174 dBm/Hz and the bandwidth to 1 MHz. The path loss parameters α_1 and α_2 are to be free space path loss with $\alpha_1 = 2$ and $\alpha_2 = \frac{1}{4\pi}$. Since we assume that the devices know their distances to the BS and their transmit power values p_i are adjusted accordingly, it is unnecessary to specify the deployment region and device deployment process. The Rayleigh fading channel parameter λ is 1, while the Nakagami fading channel parameter m is varied.

Fig. 2 shows the ratio of the achievable expected sum-rate R_o in (6) to sum-rate upper bound R in (7) for various values of r_l and the signal-to-noise ratio (SNR), while $r_h = P_{\max}$. For all SNR values, the ratio of R_o to R increases to 1 as r_l decreases. In other words, the achievable expected sum-rate approaches the sum-rate upper bound as the interference from device l to device h decreases. For any given value of r_l, the ratio of R_o to R increases as the SNR decreases. This is because lower SNR implies that the noise power is relatively stronger, and, thus, noise becomes more significant than interference as SNR decreases. Since the difference between R_o and R lies primarily in the consideration of interference from device l to device h, the ratio of R_o to R increases as the noise becomes more significant. Therefore, the sum-rate upper bound is tighter for the achievable expected sum-rate when interference is less significant and noise is more significant.

Figure 3 shows the simulated reliability for various values of t_l and m, while $t_h = P_{\max}$ and $P_{\text{th}} = 25\%$ of P_{range}. It is important to note that $m = 1$ is Rayleigh fading, and the simulated reliability with $m = 1$ matches with corresponding theoretical result in (11). For $m > 1$, the actual received powers are gamma distributed, and, thus, the simulated values of reliability for $t_l = 0$ and $t_l = t_h$ are not the same. The simulated reliability decreases and then increases as t_l increases. The simulated reliability decreases, because the peaks in probability density functions of r_l and r_h start to coincide and the likelihood of transmission failure increases as t_l increases. The simulated reliability increases for higher values of t_l, because the variance of gamma distribution separates the actual received powers and the likelihood of transmission failure decreases as t_l increases. For Nakagami-m fading with $m > 1$, reliability is higher for lower values of t_l, which implies that there is a tradeoff between reliability and sum-rate upper bound. Furthermore, for higher m, separating t_l and t_h is more important to achieve higher reliability.

Figure 4 shows the simulated reliability and sum-rate upper bound for various values of m, while $t_l = t_h$ and $P_{\text{th}} = 25\%$ of P_{range}. For Rayleigh fading channel, $t_l = t_h = P_{\max}$ is the solution that maximizes both reliability and sum-rate upper bound. For any value of m, reliability and sum-rate upper bound both increase as $t_l = t_h$ increases from $P_{\min}$ to $P_{\max}$. The simulated reliability increases, because the variance of gamma distribution increases as $t_l = t_h$ increases and it is more likely for Nakagami-m fading channel to separate the actual received powers. The simulated sum-rate upper bound increases, because the actual received powers increase as $t_l = t_h$ increases. Although there is no tradeoff between reliability and sum-rate upper bound when $t_l = t_h$, $t_l < t_h = P_{\max}$ achieves a higher reliability than $t_l = t_h = P_{\max}$ as shown in Figure 3.

Figure 5 shows the simulated reliability and sum-rate upper

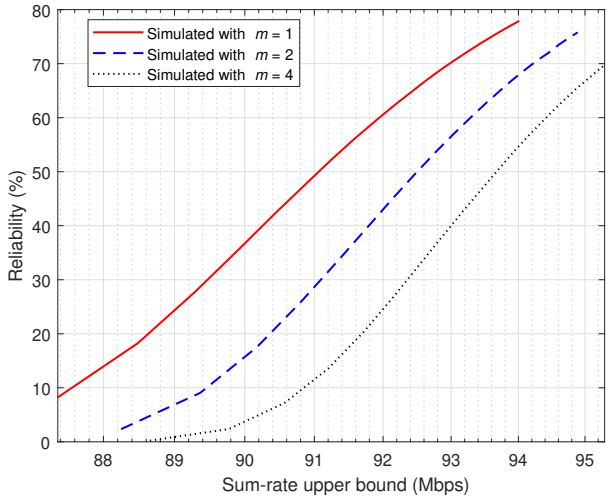

Fig. 4: Simulated reliability and sum-rate upper bound for various values of m with $t_l = t_h$ and $P_{\text{th}} = 25\%$ of P_{range}.

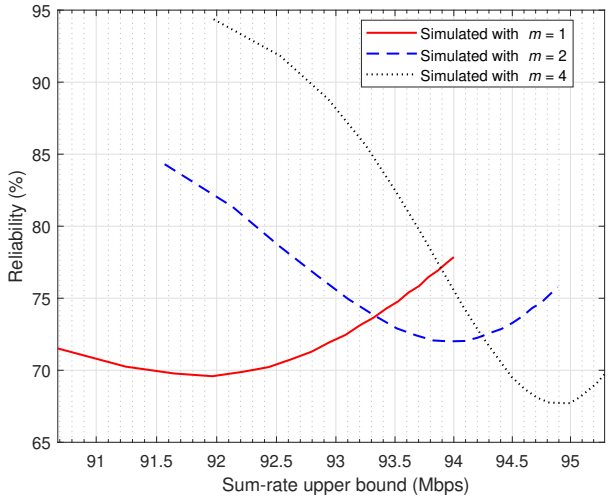

Fig. 5: Simulated reliability and sum-rate upper bound for various values of m with $t_l = P_{\text{max}}$ and $P_{\text{th}} = 25\%$ of P_{range}.

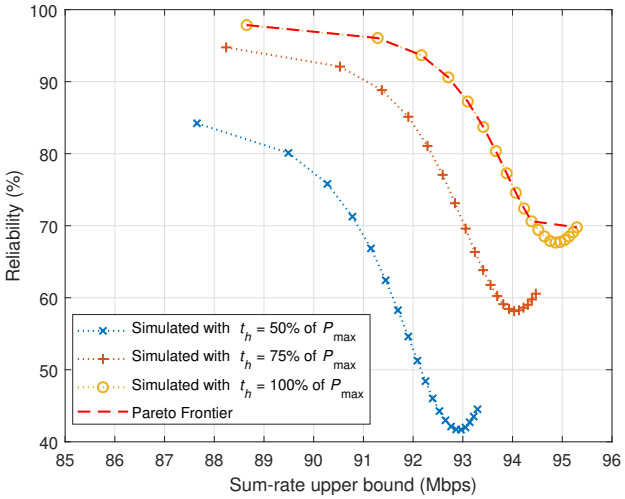

Fig. 6: Simulated reliability and sum-rate upper bound for various values of t_h with $m = 4$ and $P_{\text{th}} = 25\%$ of P_{range}.

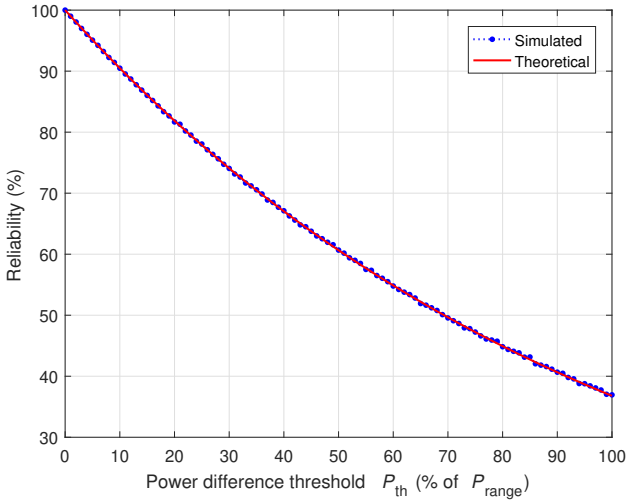

Fig. 7: Theoretical and simulated reliability for various values of P_{th} with $t_l = t_h = P_{\text{max}}$ and $m = 1$.

bound for various values of m, while $t_h = P_{\text{max}}$ and $P_{\text{th}} = 25\%$ of P_{range}. For any m, the simulated sum-rate upper bound increases as t_l increases from P_{min} to P_{max} with fixed $t_h = P_{\text{max}}$. However, for $m > 1$, $t_l = t_h = P_{\text{max}}$ does not maximize both reliability and sum-rate upper bound. For $m > 1$, the simulated reliability can increase higher by lowering sum-rate upper bound. Therefore, there is a tradeoff between reliability and sum-rate upper bound for Nakagami-m fading channel when $m > 1$ and $t_l < t_h = P_{\text{max}}$. Furthermore, the solution of $t_l = t_h = P_{\text{max}}$ is not applicable to Nakagami-m fading channel, and t_l can be chosen to satisfy given reliability and sum-rate requirements.

Figure 6 shows the simulated reliability and sum-rate upper bound for various values of t_h, while $m = 4$, $P_{\text{th}} = 25\%$ of P_{range}, and t_l increases from P_{min} to t_h. As t_l increases from P_{min} to t_h, the simulated sum-rate upper bound increases, but the reliability decreases for all values of t_h. Therefore, similar to Figure 5, there is a tradeoff between reliability and sum-rate upper bound for all values of t_h. As t_h increases, higher reliability and higher sum-rate upper bound can be achieved. Moreover, with $t_h = P_{\text{max}}$, a Pareto frontier can be found for Nakagami-m fading channel with $m = 4$. The solution of $t_l = t_h = P_{\text{max}}$ is not optimal solution to maximize reliability and sum-rate upper bound, and different pair of t_l and t_h can be chosen to satisfy given reliability and sum-rate requirements.

Figure 7 shows the theoretical and simulated reliability of PD-NOMA for various values of P_{th}, while $t_l = t_h = P_{\text{max}}$ and $m = 1$. It is important to note that P_{th} is defined as a percentage of P_{range}, and $t_l = t_h = P_{\text{max}}$ yields the highest achievable reliability. Moreover, $P_{\text{th}} = 0\%$ of P_{range} implies perfect SIC i.e., any received signals can be decoded successfully, while increasing values of P_{th} implies a worse

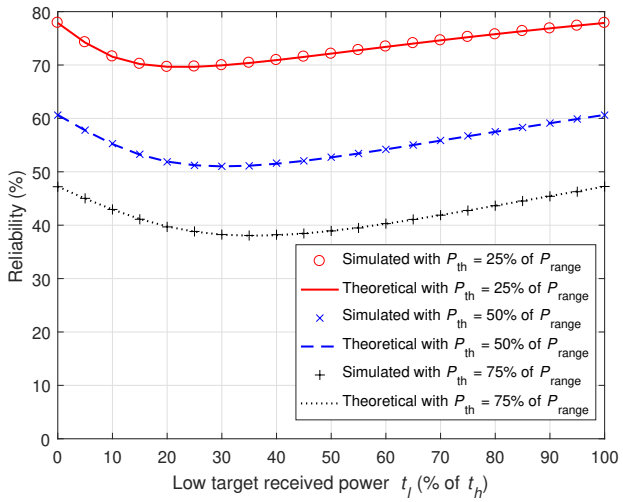

Fig. 8: Theoretical and simulated reliability for various values of t_l and P_{th} with $t_h = P_{\max}$ and $m = 1$.

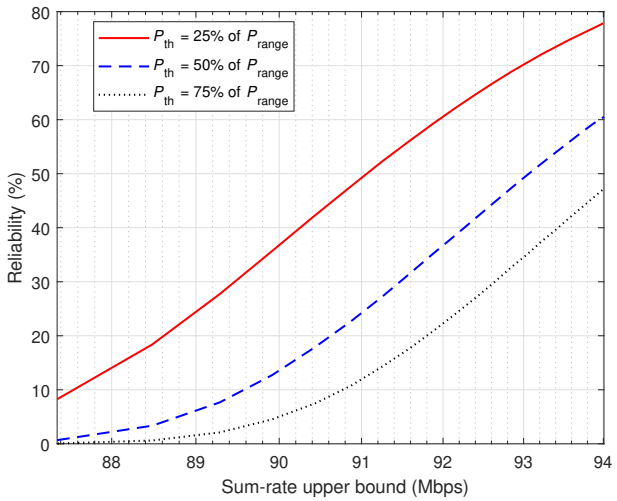

Fig. 9: Simulated reliability and sum-rate upper bound for various values of P_{th} with $t_l = t_h$ and $m = 1$.

SIC performances. For Rayleigh fading channel, the theoretical values of reliability calculated using (11) coincides closely with the simulated values of reliability. The reliability is 100% with a perfect SIC with $P_{\text{th}} = 0\%$ of P_{range}, and the reliability is 36.8% with SIC with $P_{\text{th}} = 100\%$ of P_{range}. Furthermore, the reliability decreases as the value of P_{th} increases. This is because it is less likely for the actual received power values r_l and r_h to be more than P_{th} apart for higher values of P_{th} with fixed values of t_l and t_h. As it can be seen in (27), which expresses the reliability as a function of only P_{th} when $t_l = t_h = P_{\max}$, the reliability is an exponentially decreasing function of P_{th}.

Figure 8 shows the theoretical and simulated reliability of PD-NOMA for various values of P_{th} and t_l, while $t_h = P_{\max}$ and $m = 1$. It is important to note that t_l is defined as a percentage of t_h. The highest reliability is 77.9% for $P_{\text{th}} = 25\%$ of P_{range}, 60.7% for $P_{\text{th}} = 50\%$ of P_{range}, and 47.2% for $P_{\text{th}} = 75\%$ of P_{range}. Moreover, for Rayleigh fading channel, the highest reliability occurs when $t_l = 0\%$ and $t_l = 100\%$ of t_h as proved in Proposition 2. Similar to Figure 3, the reliability initially decreases for small values of t_l, because a possibility of transmission failure due to $\Delta_r \leq P_{\text{th}}$ is introduced from device l not transmitting with $t_l = 0$. However, the reliability increases for higher values of t_l, because the variance of exponentially distributed r_l increases with increasing mean t_l. Therefore, with fixed $t_h = P_{\max}$, it is more likely for actual received powers r_i to be separated by more than P_{th}. As shown in Figure 7, the reliability increases as P_{th} decreases for corresponding values of t_l. Moreover, decreasing the value of P_{th} more effectively increases the value of reliability than changing the value of t_l.

Figure 9 shows the simulated reliability and sum-rate upper bound of PD-NOMA for various values of the sum-rate upper bound and P_{th}, while $t_l = t_h$ for the highest reliability and $m = 1$. The sum-rate upper bound increases

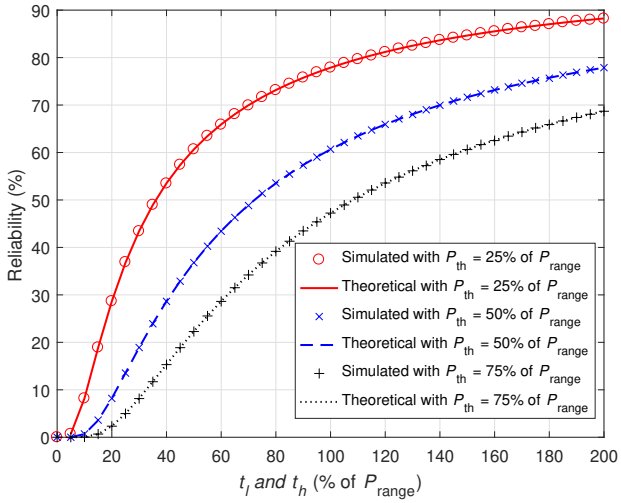

Fig. 10: Theoretical and simulated reliability for various values of t_l, t_h, and P_{th} with $t_l = t_h$ and $m = 1$.

as $t_l, t_h \in [P_{\min}, P_{\max}]$ increase. The highest sum-rate upper bound is 94 Mbps for all values of P_{th}, and this occurs when $t_l = t_h = P_{\max}$. As shown in Figure 8, the corresponding reliability for the highest sum-rate upper bound is 77.9% for $P_{\text{th}} = 25\%$ of P_{range}, 60.7% for $P_{\text{th}} = 50\%$ of P_{range}, and 47.2% for $P_{\text{th}} = 75\%$ of P_{range}. The reliability in (11) and the sum-rate upper bound in (29) are both increasing functions of t_l and t_h. Therefore, as shown in Figure 9, there is no tradeoff between the sum-rate upper bound and the reliability, when Rayleigh fading channel is considered.

Figure 10 shows the theoretical and simulated reliability for various values of t_l, t_h, and P_{th}, while $t_l = t_h$ for the highest reliability and $m = 1$. It is important to note that t_l and t_h are defined as percentages of P_{range}, since $P_{\min} = 0$ W. If $P_{\min} > 0$ W, t_l and t_h would be defined as a sum of $P_{\min}$ and percentage of P_{range} to ensure t_l and t_h are in the

bounds $[P_{\min}, P_{\max}]$. Moreover, t_l and t_h increase up to $2P_{\max}$ to analyze the reliability at higher values of target received power values. When $t_l = t_h = 2P_{\max}$, the value of reliability is 88.3% for $P_{\text{th}} = 25\%$ of P_{range}, 77.9% for $P_{\text{th}} = 50\%$ of P_{range}, and 68.74% for $P_{\text{th}} = 75\%$ of P_{range}. As t_l and t_h increase from $P_{\min}$ to $2P_{\max}$, the value of reliability increases for all P_{th}. This is because the target received power values t_i are means of the exponentially distributed actual received power values r_i with $m = 1$. When the target received power values t_i increase, the variance of the exponentially distributed actual received power also increases, because the variance is t_i^2. Therefore, with a higher t_i, it is more likely for the actual received power values r_i to be separated by more than P_{th} for successful transmission. In other words, the power separation of P_{th} required for successful decoding using SIC is done naturally by Rayleigh fading. Furthermore, Rayleigh fading is more likely to separate the actual received powers by more than P_{th} with higher target received power values. Therefore, with Rayleigh fading, it is unnecessary to allocate lower and higher target received power values. Moreover, both devices should choose the target received power values of $P_{\max}$ for the highest sum-rate upper bound and reliability.

V. Conclusion

In this paper, we have proposed a novel approach for allocating the lower and higher target received power values to IoT devices using PD-NOMA with different fading channels. In particular, we have analyzed the sum-rate upper bound and the reliability in terms of target received power values and power difference threshold for Rayleigh and Nakagami-m fading channels. Using both mathematical analysis and simulations, we have shown that the highest sum-rate upper bound and the highest reliability are achieved when the target received power values are highest for Rayleigh fading channel. Moreover, for Rayleigh fading channel, the simulation results have shown that the reliability is an increasing function of the target received power values and a decreasing function of the power difference threshold. However, we have shown that decreasing the power difference threshold is more effective in increasing the reliability than increasing the target received power values. Furthermore, we have derived the sum-rate upper bound and shown that it is an increasing function of target received power values. For Rayleigh fading channel, it is unnecessary to allocate different target received power values to the devices, because the target received power values must be highest to maximize both reliability and sum-rate upper bound. However, for Nakagami-m fading channel, we have shown that there is a tradeoff between reliability and sum-rate upper bound via simulations, and an allocation of lower and higher target received power values is necessary to satisfy the communication requirements of IoT-like services. One interesting future direction is to consider device mobility and to allocate the target power levels based on the mobility.

References

[1] S. R. Islam, N. Avazov, O. A. Dobre, and K.-S. Kwak, "Power-domain non-orthogonal multiple access (NOMA) in 5G systems: Potentials and challenges," *IEEE Communications Surveys & Tutorials*, vol. 19, no. 2, pp. 721–742, Secondquarter 2017.

[2] W. Saad, M. Bennis, and M. Chen, "A vision of 6G wireless systems: Applications, trends, technologies, and open research problems," *IEEE Network*, vol. 34, no. 3, pp. 134–142, May 2020.

[3] M. Shirvanimoghaddam, M. Dohler, and S. J. Johnson, "Massive non-orthogonal multiple access for cellular iot: Potentials and limitations," *IEEE Communications Magazine*, vol. 55, no. 9, pp. 55–61, Sep. 2017.

[4] Z. Ding, Y. Liu, J. Choi, Q. Sun, M. Elkashlan, C. L. I, and H. V. Poor, "Application of non-orthogonal multiple access in LTE and 5G networks," *IEEE Communications Magazine*, vol. 55, no. 2, pp. 185–191, Feb. 2017.

[5] X. Zhang and M. Haenggi, "The performance of successive interference cancellation in random wireless networks," *IEEE Transactions on Information Theory*, vol. 60, no. 10, pp. 6368–6388, Oct 2014.

[6] A. E. Mostafa, Y. Zhou, and V. W. Wong, "Connectivity maximization for narrowband IoT systems with NOMA," in *Proc. of IEEE International Conference on Communications*, Paris, France, May 2017, pp. 1–6.

[7] M. Baghani, S. Parsaeefard, M. Derakhshani, and W. Saad, "Dynamic non-orthogonal multiple access and orthogonal multiple access in 5G wireless networks," *IEEE Transactions on Communications*, vol. 67, no. 9, pp. 6360–6373, Sep. 2019.

[8] Z. Yang, Z. Ding, P. Fan, and N. Al-Dhahir, "A general power allocation scheme to guarantee quality of service in downlink and uplink noma systems," *IEEE Transactions on Wireless Communications*, vol. 15, no. 11, pp. 7244–7257, Aug. 2016.

[9] S. Chen, K. Peng, and H. Jin, "A suboptimal scheme for uplink NOMA in 5G systems," in *Proc. of International Wireless Communications and Mobile Computing Conference*, Dubrovnik, Croatia, Aug. 2015, pp. 1429–1434.

[10] S. A. R. Naqvi and S. A. Hassan, "Combining NOMA and mmWave technology for cellular communication," in *Proc. of IEEE Vehicular Technology Conference*, Montreal, QC, Canada, Sep. 2016, pp. 1–5.

[11] J. N. Chattha and M. Uppal, "Relay-aided non-orthogonal multiple access with noisy network coding," in *Proc. of IEEE International Conference on Communications*, Paris, France, May 2017, pp. 1–6.

[12] L. Salaün, C. S. Chen, and M. Coupechoux, "Optimal joint subcarrier and power allocation in NOMA is strongly NP-hard," in *Proc. of IEEE International Conference on Communications*, Kansas City, USA, May 2018, pp. 1–7.

[13] C. Wang, Y. Chen, Y. Wu, and L. Zhang, "Performance evaluation of grant-free transmission for uplink URLLC services," in *Proc. of IEEE Vehicular Technology Conference*, Sydney, Australia, June 2017, pp. 1–6.

[14] T. Park, G. Lee, and W. Saad, "Message-aware uplink transmit power level partitioning for non-orthogonal multiple access (NOMA)," in *Proc. of IEEE Global Communications Conference*, Abu Dhabi, UAE, Dec. 2018, pp. 1–6.

[15] E. Balevi, F. T. A. Rabee, and R. D. Gitlin, "ALOHA-NOMA for massive machine-to-machine IoT communication," in *Proc. of IEEE International Conference on Communications*, Missouri, USA, May 2018, pp. 1–5.

[16] M. Basharat, W. Ejaz, M. Naeem, A. M. Khattak, A. Anpalagan, and O. Alfandi, "Energy efficient resource allocation for NOMA in cellular iot with energy harvesting," in *Proc. of International Conference on Emerging Technologies*, Islamabad, Pakistan, Dec. 2017, pp. 1–6.

[17] D. Zhai, R. Zhang, L. Cai, B. Li, and Y. Jiang, "Energy-efficient user scheduling and power allocation for NOMA-based wireless networks with massive IoT devices," *IEEE Internet of Things Journal*, vol. 5, no. 3, pp. 1857–1868, Jun. 2018.

[18] R. Abozariba, M. K. Naeem, M. Patwary, M. Seyedebrahimi, P. Bull, and A. Aneiba, "NOMA-based resource allocation and mobility enhancement framework for IoT in next generation cellular networks," *IEEE Access*, vol. 7, pp. 29 158–29 172, Jan. 2019.

[19] M. Shirvanimoghaddam, M. Condoluci, M. Dohler, and S. J. Johnson, "On the fundamental limits of random non-orthogonal multiple access in cellular massive IoT," *IEEE Journal on Selected Areas in Communications*, vol. 35, no. 10, pp. 2238–2252, Oct. 2017.

[20] Z. Ma, M. Xiao, Y. Xiao, Z. Pang, H. V. Poor, and B. Vucetic, "High-reliability and low-latency wireless communication for internet of things: Challenges, fundamentals, and enabling technologies," *IEEE Internet of Things Journal*, vol. 6, no. 5, pp. 7946–7970, Oct. 2019.

[21] C. Chaccour, M. N. Soorki, W. Saad, M. Bennis, and P. Popovski, "Can terahertz provide high-rate reliable low latency communications for wireless VR?" , *arXiv:2005.00536*, 2020.
[22] D. Zwillinger, *Table of integrals, series, and products*. Elsevier, 2014.